AGU100 ADVANCING EARTH AND SPACE SCIENCE

Geophysical Research Letters

RESEARCH LETTER
10.1029/2018GL079715

**Key Points:**
- Feedback instability in the magnetosphere-ionosphere coupling is unstable even in a case with strong vertical flow shear in the *E* layer
- The linear eigenmode analysis captures entire profiles of the electromagnetic fields and the density perturbations along a field line
- A conventional magnetosphere-ionosphere coupling model with a height-integrated ionosphere remains valid in a low-frequency regime

**Correspondence to:**
T.-H. Watanabe,
watanabe.tomohiko@nagoya-u.jp

**Citation:**
Watanabe, T.-H., & Maeyama, S. (2018). Unstable eigenmodes of the feedback instability with collision-induced velocity shear. *Geophysical Research Letters*, *45*, 10,043–10,049. https://doi.org/10.1029/2018GL079715

Received 20 JUL 2018
Accepted 13 SEP 2018
Accepted article online 19 SEP 2018
Published online 2 OCT 2018



# Unstable Eigenmodes of the Feedback Instability With Collision-Induced Velocity Shear

**T.-H. Watanabe[1] and S. Maeyama[1]**

[1] Department of Physics, Nagoya University, Nagoya, Japan

**Abstract** A linear eigenmode analysis of the magnetosphere-ionosphere coupling shows that the feedback instability leading to spontaneous formation of auroral arc structures remains unstable even in a case with strong vertical shear of horizontal ion flows induced by ion-neutral collisions in the *E* layer. For low-order Alfvén harmonics, the linear frequency and growth rate obtained by means of a height-resolved model of the ionosphere are comparable to those resulted from the height-integrated one, where fine vertical structures of the ionospheric density and magnetic field perturbations are well resolved in the former. The present result confirms validity of the height-integrated ionosphere model in the long parallel wavelength limit, as assumed in previous studies on the feedback instability.

**Plain Language Summary** Spontaneous formation of auroral arcs can be explained in terms of a plasma instability in the magnetosphere-ionosphere coupling. The present study confirms validity and robustness of the basic instability theory even in cases with inhomogeneous profiles of the ionospheric parameters such as the ion-neutral collision.

## 1. Introduction

The magnetosphere-ionosphere (M-I) coupling is considered to play a key role in auroral phenomena observed in polar regions. Specifically, the Alfvénic interactions of the magnetosphere and the ionosphere are important not only to the energy transfer associated with the equilibrium current system but also to time variations and fine structuring of auroras. The feedback M-I coupling has been considered as one of the plausible mechanisms to describe spontaneous formation of auroral arc structures (Atkinson, 1970; Sato, 1978), where ionospheric density perturbations are coupled with local circuits of the ionospheric current and the field-aligned and polarization currents carried by shear Alfvén waves and can grow if the background electric field exceeds a critical value. Since then, a variety of linear and nonlinear analyses on the feedback instability have been carried out for the field-line-resonance scale interactions (Lu et al., 2007, 2008; Miura & Sato, 1980; Watanabe, 2010; Watanabe & Sato, 1988; Watanabe et al., 1993), of which time scale is a few minutes, as well as for the ionospheric cavity-type modes (Lysak, 1991; Pokhotelov et al., 2000, 2001; Streltsov & Lotko, 2003, 2004, 2008) and their hybrid mode (Hiraki & Watanabe, 2011, 2012). More recent developments include the gyrokinetic model (Watanabe, 2014) and transition to the Alfvénic turbulence (Watanabe et al., 2016) for the feedback M-I coupling. The M-I coupling model for the feedback instability analysis is facilitated with the height-integrated ionosphere, because the effective height of the ionospheric *E* layer is negligibly shorter than field line length of the Alfvénic oscillation and is likely to be smaller than the wavelength of the ionospheric cavity mode. However, a recent analysis including the ionospheric inhomogeneity has questioned validity of the height-integrated model and the feedback instability growth (Sydorenko & Rankin, 2017), where collision-induced vertical shear of a horizontal ion flow inside of the *E* layer is considered to prevent amplification of the density perturbation, not only for the high-frequency ionospheric cavity-type interactions but also for the low-frequency field-line-resonance scale coupling. The present study is devoted to verification of the M-I coupling theory and demonstration of a linearly unstable eigenmode solution in a case with the inhomogeneous ionosphere model.

Recently, the M-I coupling model including the ionospheric inhomogeneity is formulated by a set of two fluid equations with effects of ion-neutral collisions, and the initial value problem was solved, where the governing equations with initial density perturbations are numerically time advanced for a finite period (Sydorenko & Rankin, 2017). The numerical results for the inhomogeneous ionosphere model did not show growth of the initial perturbation. Nevertheless, the analysis by Sydorenko and Rankin does not exclude possibility that linear unstable solutions may exist even in cases with strong ionospheric inhomogeneity, since their initial condition was arbitrary chosen and likely dissimilar from the linear eigenfunction. In the present work, we have found that there exist linearly unstable eigenmode solutions of the feedback M-I coupling even in a case with strong ionospheric inhomogeneity of the collision frequency and the Pedersen mobility and that the height-integrated approach remains to be valid in a limit of long field-aligned wavelengths of the shear Alfvén modes.

Remainder of the paper is organized as follows. The next section explains a theoretical model for the feedback instability analysis with the ionospheric inhomogeneity. Our model is based on the magnetohydrodynamic (MHD) equations extended with the Pedersen mobility of ions. The electron inertia and the displacement current included in the model by Sydorenko and Rankin (2017) are neglected here, since their contributions are minor in a low-frequency regime. Instead, we assume the quasi-neutrality. Results of the eigenmode analysis are shown in section 3, where one finds the unstable eigenmode solutions with positive growth rates. Conclusions and discussions are given in section 4.

## 2. Model

We consider a linearized set of the reduced MHD model for the shear Alfvén waves extended to involve the ionospheric plasma where the ion-neutral collisions may dominate the ion gyromotion. The MHD part obeys the same ordering as that employed for the shear Alfvén law (Hazeltine & Meiss, 1992; Watanabe, 2010). The M-I coupling system is assumed to be two-dimensional with a uniform background magnetic field. The model equations are derived by taking a low-frequency limit of the two fluid equations (Sydorenko & Rankin, 2017), where the Faraday's and Ampére's laws are written as

$$\frac{\partial B_x}{\partial t} = \frac{\partial E_y}{\partial z}\,, \tag{1}$$

$$-\frac{\partial B_x}{\partial y} = \mu_0 j_z\,, \quad \frac{\partial B_x}{\partial z} = \mu_0 j_y\,, \tag{2}$$

in the two-dimensional plane. The horizontal and vertical directions are set in the $y$ and $z$ coordinates, respectively, and the translational symmetry is assumed in the $x$ direction. We assume that the parallel current ($j_z$) along the background magnetic field ($B_0$) is carried by electrons, while the perpendicular current ($j_y$) is caused by cross-field motion of ions, such that

$$j_y = en_0 u_{iy} + en_{i1} u_{i0}\,, \tag{3}$$

$$j_z = -en_0 u_{ez}, \tag{4}$$

where $n_0$ and $n_{i1}$ are the equilibrium and the perturbed number density. The ion charge is $+e$. The zeroth- and first-order components of ion flow velocity are given by

$$u_{i0} = \mu_P E_0\,, \tag{5}$$

$$u_{iy} = \frac{F}{\Omega_i B_0}\frac{\partial E_y}{\partial t} + \mu_P E_y - D_i \frac{\partial}{\partial y}\left(\frac{n_{i1}}{n_0}\right), \tag{6}$$

where $E_0$ and $E_y$ are the uniform and the perturbed electric field in the $y$ direction. Two important parameters are involved in equation (6), that is, the ratio of the ion-neutral collision ($\nu_{in}$) to the ion gyrofrequency ($\Omega_i$) and the Pedersen mobility ($\mu_P$). $D_i$ means the collisional diffusion coefficient. The first term on the right in equation (6) denotes the polarization drift of ions, where the numerator defined by

$$F = \frac{1-(\nu_{in}/\Omega_i)^2}{[1+(\nu_{in}/\Omega_i)^2]^2} \tag{7}$$

varies with the ratio of $\nu_{in}$ to $\Omega_i$. One finds that $F \to 1$ for $\nu_{in}/\Omega_i \to 0$ in a collisionless plasma, while $F \to 0$ for $\nu_{in}/\Omega_i \to \infty$ in a collision-dominated plasma. The continuity equations of ion and electron number density are linearized as

$$\frac{\partial n_{i1}}{\partial t} + n_0\frac{\partial u_{iy}}{\partial y} + u_{i0}\frac{\partial n_{i1}}{\partial y} = -2\alpha n_0 n_{i1}, \tag{8}$$

$$\frac{\partial n_{e1}}{\partial t} + \frac{\partial}{\partial z}(n_0 u_{ez}) = -2\alpha n_0 n_{e1}, \tag{9}$$

where the terms on the right represent the recombination loss. By requiring the quasi-neutrality condition,

$$n_{i1} = n_{e1} \equiv n_1 \tag{10}$$

the above set of equations satisfies the charge conservation ($\nabla \cdot \boldsymbol{j} = 0$) and is self-consistently closed. The nonideal MHD effects are deleted by substituting $\nu_{in} = \mu_P = D_i = \alpha = 0$, and one finds the linearized ideal MHD equations and the constant density. In the present study, we assume the periodic boundary condition in the $y$ direction and set the origin of the $z$ coordinate at the top of $E$ layer. The perturbed quantities in equations (1)–(9) are assumed to have the wave number $k_y$ and the frequency $\omega$, that is, $\propto \exp(ik_y y - i\omega t)$ and are Fourier transformed in $y$ and $t$. The Fourier mode amplitudes are denoted by $\tilde{B}_x(z)$, $\tilde{E}_y(z)$, and $\tilde{n}_1(z)$ and are functions of $z$. Then, one finds that

$$\left(\omega - k_y\mu_P E_0 + i2\alpha n_0 + ik_y^2 D_i\right)\frac{\mathrm{d}\tilde{B}_x}{\mathrm{d}z} = -\left(\omega + i2\alpha n_0\right)\left(i\omega\frac{F}{V_A^2} - \mu_0\sigma_P\right)\tilde{E}_y \tag{11}$$

$$\frac{\mathrm{d}\tilde{E}_y}{\mathrm{d}z} = -i\omega\tilde{B}_x\,. \tag{12}$$

$V_A$ and $\sigma_P$ on the right of equation (11) are the Alfvén velocity $V_A = B_0/\sqrt{\mu_0 m_i n_0}$ and the Pedersen conductivity $\sigma_P = e\mu_P n_0$, where $m_i$ means the ion mass. The set of ordinary differential equations for $z$, equations (11) and (12), can be solved as an eigenvalue problem, when an appropriate boundary condition is provided. If the complex-valued eigenfrequency $\omega$ has a positive imaginary part, the eigenmode grows exponentially in time. Here it is instructive to see that equations (11) and (12) result in the simple wave equation in the ideal MHD limit,

$$\frac{\mathrm{d}\tilde{B}_x}{\mathrm{d}z} = -\frac{i\omega}{V_A^2}\tilde{E}_y\,,\quad \frac{\mathrm{d}\tilde{E}_y}{\mathrm{d}z} = -i\omega\tilde{B}_x\,. \tag{13}$$

Since a geometry of the system is assumed to be uniform in the present study, the $z$ dependence of the mode amplitude stems from physical parameters varying along the field line, $n_0 = n_0(z)$, $V_A = V_A(z)$, $\mu_P = \mu_P(z)$, $\nu_{in} = \nu_{in}(z)$, $\alpha = \alpha(z)$, and $D_i = D_i(z)$. Thus, $F$ and $\sigma_P$ also depend on $z$, $F = F(z)$, and $\sigma_P = \sigma_P(z)$.

Assuming the system to be symmetric for the both hemispheres, we focus on a symmetric (antisymmetric) solution for $E_y$ ($B_x$) with respect to the magnetic equator at $z = l$, while extension to the antisymmetric (symmetric) case for $E_y$ ($B_x$) is straightforward. The lower boundary for the bottom of $E$ layer is set at $z = -h$, where the perturbed component of magnetic field ($B_x$) vanishes.

In the following, we consider a simple model to include the collision-induced velocity shear in the M-I feedback coupling. We assume the uniform background density $n_0$ and the Alfvén speed $V_A = V_{A0}$, but strong inhomogeneity is introduced in $\mu_P$ and $\nu_{in}$, such that

$$\mu_P(z) = \begin{cases} 0 & \text{if } 0 \le z \le l \\ \frac{\nu_{in}/\Omega_i}{B_0(1+\nu_{in}^2/\Omega_i^2)} & \text{if } -h \le z < 0 \end{cases}, \tag{14}$$

where

$$\nu_{in}(z) = \begin{cases} 0 & \text{if } 0 \le z \le l \\ \overline{\nu}_{in}\left(1 - \cos\frac{\pi z}{h}\right) & \text{if } -h \le z < 0 \end{cases}. \tag{15}$$

For simplicity we set $\alpha = D_i = 0$ in the present study. Use of the model for $\mu_P(z)$ and $\nu_{in}(z)$ given above simplifies the numerical treatment, since equations (11) and (12) reduce to the ideal MHD model for $z \ge 0$.

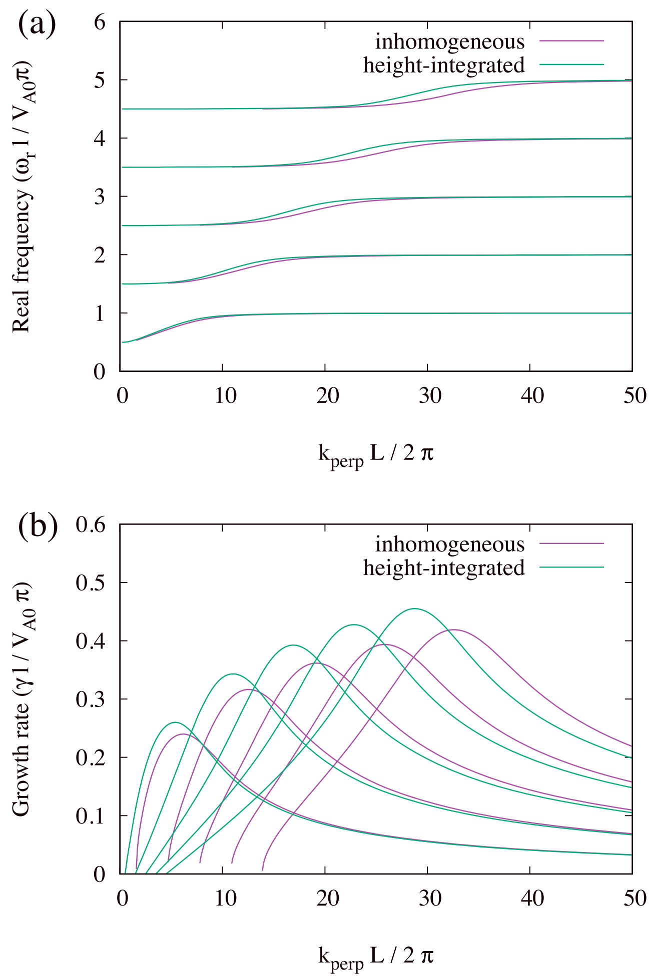


**Figure 1.** (a) Real and (b) imaginary parts of the eigenfrequency obtained by numerically solving the eigenvalue equations for the feedback instability with inhomogeneous (purple) and the height-integrated (green) ionospheric models. Lines in each plot represent lowest five Alfvén harmonics.

Normalization units are a horizontal scale length $L$, a characteristic Alfvén velocity $V_{A0}$, and the background magnetic field $B_0$. The normalized set of equations reads

$$\left(\hat{\omega} - \hat{k}_y \hat{\mu}_P \hat{E_0} + i2\hat{\alpha} + i\hat{k}_y^2 \hat{D}_i\right) \frac{\mathrm{d}\hat{B}_x}{\mathrm{d}\hat{z}} = -\frac{1}{\hat{V}_A^2} (\hat{\omega} + i2\hat{\alpha}) \left(i\hat{\omega}F - \hat{\Sigma}_0 \hat{\mu}_P\right) \hat{E}_y, \tag{16}$$

$$\frac{\mathrm{d}\hat{E}_y}{\mathrm{d}\hat{z}} = -i\hat{\omega}\hat{B}_x. \tag{17}$$

Here a nondimensional parameter $\hat{\Sigma}_0$ appearing in the Pedersen conductivity term in equation (16) is given by $\hat{\Sigma}_0 = L\Omega_i / V_{A0} = en_0 B_0^{-1} L \mu_0 V_{A0}$, that is, a product of the characteristic impedance of the magnetospheric plasma ($\mu_0 V_{A0}$) and the ionospheric Hall conductivity (as $\mu_H = B_0^{-1}$) integrated over $L$.

## 3. Results

We numerically solve the eigenvalue problem for the feedback M-I coupling as follows. One finds that equation (13) can be applied to the model magnetosphere of $0 \le z \le l$, where $\mu_P = \nu_{in} = 0$ in the present model of equations (14) and (15). The numerical solution in the magnetosphere is connected to that of equations (11) and (12) in the model ionosphere of $-h \le z < 0$ for the height-resolved model, while the ionospheric dispersion relation is used for the height-integrated case. Starting from an initial estimate of $\omega$ for a given value of $k_y$, the numerical integration is carried out from $z = l$ to $z = -h$ by means of the

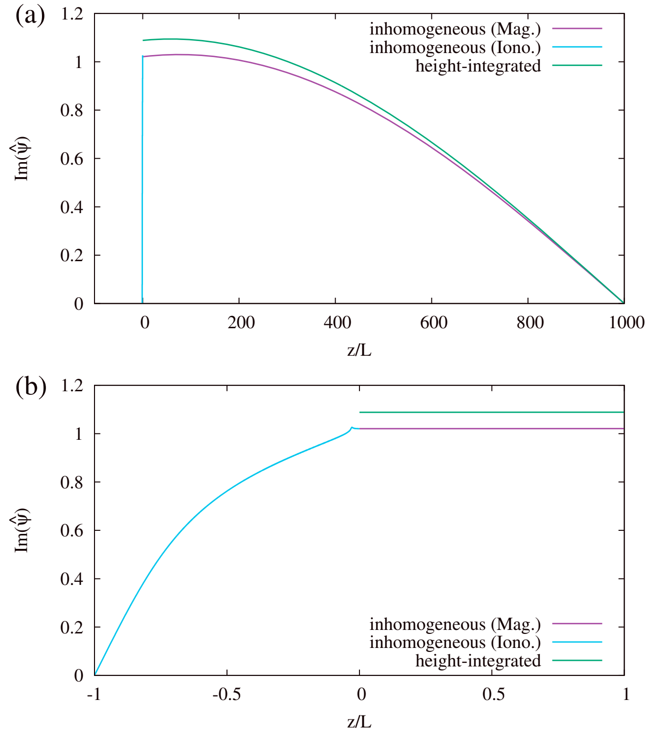


**Figure 2.** Imaginary part of the eigenfunction for the magnetic flux $\hat{\Psi}$ of $k_y L = 4\pi$ for the inhomogeneous (purple and light blue for $0 \le z \le l$ and $-h \le z < 0$, respectively, where $l = 1,000$ and $h = 1$) and the height-integrated (green) ionospheric models. Panel (a) shows the whole profile, and the magnified plots for a range of $-h < z < h$ are shown in panel (b). A steep gradient of $\psi_k$ inside of the ionosphere is well captured in the inhomogeneous case.

fourth-order Runge-Kutta method. If the magnetic perturbation at the bottom of the ionosphere does not satisfy the boundary condition of $\tilde{B}_x(z = -h) = 0$, we recompute the numerical integration with a correction to $\omega$. The procedure is iterated by using Newton's method until the boundary condition is fulfilled. Then we find the dispersion relation by scanning $k_y$. We employed 500 grid points for $0 \le z \le l$ and 2,000 grid points for $-h \le z < 0$ so that the strong inhomogeneity in the $E$ layer can be accurately resolved.

In the present analysis we used the following parameters: $l = 1,000L$, $h = L$, $\overline{\mu}_P E_0 = 5 \times 10^{-4} V_{A0}$, $\overline{\mu}_P B_0 \hat{\Sigma}_0 = 5$, and $\overline{\nu}_{in} = 10\Omega_i$, where $\overline{\mu}_P$ means the height average of $\mu_P(z)$ in equation (14) from $z = -h$ to 0; that is, $\overline{\mu}_P B_0 = 0.154$ for the present model of $\nu_{in}/\Omega_i$. The height-resolved $\mu_P(z)B_0$ has its peak value of $\mu_P(z)B_0 = 0.5$, where $\nu_{in}/\Omega_i = 1$, that is, at $z = -0.144L$ for the present case. These parameters are determined in reference to our previous work (Watanabe, 2010) while we set $\alpha = 0$ and $D_i = 0$ for simplicity.

Numerical results of the eigenvalue analysis are shown in Figure 1, where (a) real and (b) imaginary parts of the eigenfrequency $\omega = \omega_r + i\gamma$ are plotted for cases with the height-integrated and inhomogeneous ionospheric models. Plots of $\omega_r$ for the both cases clearly show the Alfvén harmonics for the five lowest branches with positive-valued $\omega_r$ and $k_y$. The imaginary part of $\omega$ shows existence of unstable modes with positive growth rates for all harmonics, where the larger maximum growth rates are found for higher harmonics. It is important to note that all modes involve unstable solutions even in the case with the strong ionospheric inhomogeneity of the Pedersen mobility and the ion-neutral collision frequency. Although magnitudes of the maximum growth rates in the inhomogeneous case are slightly reduced (about 8% reduction) in comparison to those of the height-integrated model, the unstable eigenmodes grow exponentially in time with the characteristic time scales of $\gamma^{-1}$ which is of the order of several Alfvén transit times ($l/V_{A0}$) between the ionosphere and the magnetic equator. We have confirmed that the linear growth rates are insensitive to a change of the ionospheric height $h$ at least within a factor of 5 (that is, from $h = L/5$ to $5L$).

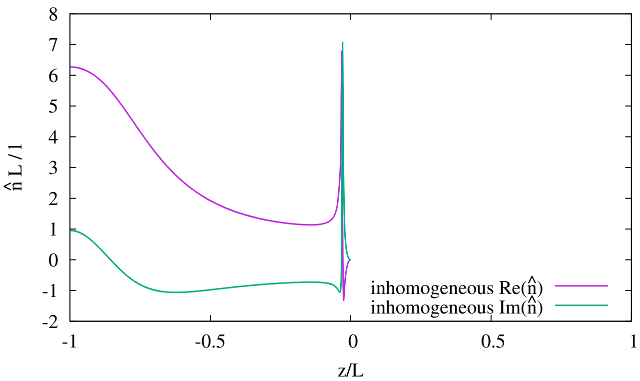


**Figure 3.** Eigenfunction of the number density $\hat{n}$ of $k_y L = 4\pi$ for the inhomogeneous ionospheric model plotted for $-h \le z < 0$. No density perturbation arises in the magnetosphere ($z \ge 0$) where the collision-related parameters are set to be zero in the present model ($\mu_P = 0$ and $\nu_{in} = 0$).

An eigenmode structure of the unstable solution is shown in Figure 2, where the imaginary part of the magnetic flux function, $\hat{\psi} = -i\hat{B}_x/\hat{k}_y$, is plotted for $\hat{k}_y = k_y L = 4\pi$ in the lowest branch of $\omega_r$. Amplitude of the linear eigenfunction is normalized so that the electric potential $\hat{\phi} = i\hat{E}_y/\hat{k}_y = 1$ at $z = l$. The eigenfunctions in the magnetosphere ($z > 0$) are quite similar to each other for the height-integrated and inhomogeneous ionosphere models. However, a very sharp drop of the magnetic field perturbation amplitude in the ionosphere appears in the latter, because of the boundary condition of $\tilde{B}_x = 0$ at the bottom of the ionosphere ($z = -h$), while the amplitude of $\hat{\phi}$ (and hence, $\tilde{E}_y$) keeps almost constant in the ionosphere. It is noteworthy that the steep gradient of the mode structure is successfully captured as shown in the magnified plots in Figure 2b, since enough numerical resolution is employed for the ionosphere.

The inhomogeneous ionospheric structure is also reflected to the eigenfunction of density perturbation. The vertical profile of $\hat{n} = \tilde{n}_1/n_0$, of which amplitude is normalized as $\hat{\phi}(z = l) = 1$, is plotted in Figure 3 for $-h < z < 0$. The density perturbation in the magnetosphere of $z \ge 0$ vanishes as $\mu_P = \nu_{in} = 0$ and is not plotted there. Sharp peaks appear at $z \approx -0.03L$, which is attributed to a resonant interaction of the shear Alfvén wave and the ionospheric Pedersen flow, provided by $\omega - k_y \mu_P E_0 \approx 0$ in equation (11). The resonant mode structure is due to the collision-induced flow shear. It is, thus, clear that the present model is accompanied with the quite strong shear flow effect. We have also found that the resonant mode structure is relaxed by introduction of the finite recombination ($\alpha$) or diffusion ($D_i$). The above analysis confirms that the feedback interaction robustly works in the M-I coupling even with the ionospheric inhomogeneity, leading to exponential growth of the linearly unstable eigenmode solution.

## 4. Conclusion and Discussion

We have investigated the feedback coupling of the magnetosphere and the ionosphere with effects of collision-induced velocity shear of horizontal ion flows. Theoretical and numerical analyses of our model including the strong vertical inhomogeneity of the Pedersen mobility and the ion-neutral collision frequency have clearly demonstrated robustness of the feedback instability, indicating existence of the linear unstable eigenmode. It is noteworthy that the unstable solutions do exist even in a case with the inhomogeneous ionospheric parameters, although the linear growth rates are slightly reduced in comparison to those obtained from the height-integrated model. The obtained result showing little influence of the ionospheric inhomogeneity on the feedback coupling in a low-frequency range is attributed to the nearly constant amplitude of electric potential perturbations in the ionosphere. It is considered to reflect a general feature of long wavelength perturbations which can propagate beyond a barrier with a steep but short-scale change of parameters in analogy to the tunneling effect in quantum mechanics.

Here we remark the normalization units and parameters employed in the present model. Let us assume $L =$ 50 km and $V_{A0} = 1,000$ km/s for a rough estimate of parameters, such as $l = 5 \times 10^4$ km and the Alfvén transit time $\tau_A = l/V_{A0} = 50$ s. The perpendicular wavelength is 25 km for $k_\perp L = 4\pi$ (of which eigenfunctions are shown in Figures 2 and 3) and 8.3 km for $k_\perp L = 12\pi$. The latter corresponds to the most unstable mode in the lowest Alfvén harmonics. The typical growth time is characterized by the inverse of the linear growth rate $\gamma$. For the most unstable mode in the lowest Alfvén harmonics with $k_\perp L = 12\pi$, $\gamma^{-1} = (0.75V_{A0}/l)^{-1} = 66.6$ s (i.e., $\gamma = 0.015$ s$^{-1}$). Also, the used parameter of $\bar{\mu}_P B_0 \hat{\Sigma}_0 = 5$ means the height-integrated Pedersen conductance of $\Sigma_P \equiv e n_0 \bar{\mu}_P h = 5h/L\mu_0 V_{A0} = 4$ mho for $h = L$, while the estimate of $\Sigma_P$ may be varied by the assumed value of $V_{A0}$.

The normalized and height-averaged Pedersen mobility of $\bar{\mu}_P B_0 = 0.154$ gives a rather large value of $\hat{\Sigma}_0 = 32.5$ for $\bar{\mu}_P B_0 \hat{\Sigma}_0 = 5$ if we assume $B_0 = 5 \times 10^{-5}$ T. In the present case, however, $\bar{\mu}_P B_0$ is given by the model collisionality where strong inhomogeneity of $\nu_{in}(z)$ is introduced with $\bar{\nu}_{in} = 10\Omega_i$ in order to clearly demonstrate existence of the unstable eigenmode solution in the height-resolved ionosphere. For a rather modest value of $\bar{\nu}_{in} = 2\Omega_i$, one finds $\bar{\mu}_P B_0 = 0.303$ and $\hat{\Sigma}_0 = 16.5$ for $\bar{\mu}_P B_0 \hat{\Sigma}_0 = 5$. We have also found that the linear frequency and growth rate for the feedback instability are only slightly influenced for the change of $\bar{\nu}_{in}$ from $\bar{\nu}_{in}/\Omega_i = 10$ to 2. It may also be meaningful to reconfirm that the feedback instability can grow under a realistic condition with a stabilizing effect of the recombination loss. Even in a case with high electron number density of $n_0 = 10^{11}$ m$^{-3}$, $\alpha n_0 \approx 8\times10^{-3}$ s$^{-1}$ for the recombination rate of $\alpha \approx 0.8\times10^{-13}$ m$^3$/s (for $O_2^+$ with the electron temperature of 1000 °K; Torr et al, 1976). In the normalization unit used here, $\alpha n_0 L/V_{A0} \approx 4\times10^{-4}$, while we have found the feedback instability growth even with a stronger recombination effect of $\alpha n_0 L/V_{A0} \approx 7\times10^{-4}$ (Watanabe, 2010; also, Sato had shown the feedback instability for $\alpha = 3\times10^{-13}$ m$^3$/s and $n_0 = 5\times10^9$ m$^{-3}$ in the original paper; Sato, 1978).

The present results shown in the previous section are in contrast to the recent work by Sydorenko and Rankin (2017) where they concluded stabilization of the feedback instability due to the collision-induced flow shear in the ionosphere. Two possible reasons may be considered for the different conclusions. First, we have discussed the M-I coupling via the Alfvén waves of which parallel wavelengths are of the order of the field line lengths, while the feedback coupling in much higher-frequency range was mainly discussed by Sydorenko and Rankin. Indeed, they introduced inhomogeneous profiles of plasma density not only in the ionosphere but also in the magnetosphere, leading to high-frequency Alfvénic coupling. The eigenmode analysis for the ionospheric cavity modes is necessary for more direct comparisons. The other possibility is due to the difference in the approach to the problem. Sydorenko and Rankin solved the initial value problem, while the eigenmode solutions are discussed in the present work. If the numerical time integration is started with an initial condition apart from the eigenfunction and carried out only for a limited period, the eigenmode solution does not have enough time to grow to a visible amplitude while most of the initial perturbations far from the eigenfunction of unstable modes will be damped.

In the present study, we discussed an idealized model while keeping essence of the ionospheric inhomogeneity with the collision-induced shear flow. More detailed studies on the parameter dependence, effects of the Hall current, and the nonlinear evolution will be pursued in future works.

**Acknowledgments**
This work was partially supported by collaboration research programs of the National Institute for Fusion Science and Institute for Space-Earth Environmental Research. No observation nor experimental data are used in the paper. A numerical dispersion relation solver used to produce Figures 1, 2, and 3 is accessible through GitHub (th-watanabe/Disp_solv_fbi_inhomo_iono).

## References

Atkinson, G. (1970). Auroral arcs: Result of the interaction of a dynamic magnetosphere with the ionosphere. *Journal of Geophysical Research*, *75*, 4746–4755. https://doi.org/10.1029/JA075i025p04746

Hazeltine, R. D., & Meiss, J. D. (1992). *"Plasma confinement"*. Redwood City: Addison-Wesley. Chap.7.

Hiraki, Y., & Watanabe, T.-H. (2011). Feedback instability analysis for dipole configuration with ionospheric and magnetospheric cavities. *Journal of Geophysical Research*, *116*, A11220. https://doi.org/10.1029/2011JA016721

Hiraki, Y., & Watanabe, T.-H. (2012). Hybrid Alfvén resonant mode generation in the magnetosphere-ionosphere coupling system. *Physics of plasmas*, *19*, 102904.

Lu, J. Y., Rankin, R., Marchand, R., Rae, I. J., Wang, W., Solomon, S., et al. (2007). Electrodynamics of magnetosphere-ionosphere coupling and feedback on magnetospheric field line resonances. *Journal of Geophysical Research*, *112*, A10219. https://doi.org/10.1029/2006JA012195

Lu, J. Y., Wang, W., Rankin, R., Marchand, R., Lei, J., Solomon, S. C., et al. (2008). Electromagnetic waves generated by ionospheric feedback instability. *Journal of Geophysical Research*, *113*, A05206. https://doi.org/10.1029/2007JA012659

Lysak, R. L. (1991). Feedback instability of the ionospheric resonant cavity. *Journal of Geophysical Research*, *96*, 1553–1568. https://doi.org/10.1029/90JA02154

Miura, A., & Sato, T. (1980). Numerical simulation of global formation of auroral arcs. *Journal of Geophysical Research*, *85*, 73–91. https://doi.org/10.1029/JA085iA01p00073

Pokhotelov, O. A., Khruschev, V., Parrot, M., Senchenkov, S., & Pavlenko, V. P. (2001). Ionospheric Alfvén resonator revisited: Feedback instability. *Journal of Geophysical Research*, *106*(25), 25,813–25,824. https://doi.org/10.1029/2000JA000450

Pokhotelov, O. A., Pokhotelov, D., Streltsov, A., Khruschev, V., & Parrot, M. (2000). Dispersive ionospheric Alfvén resonator. *Journal of Geophysical Research*, *105*, 7737–7746. https://doi.org/10.1029/1999JA900480

Sato, T. (1978). A theory of quiet auroral arcs. *Journal of Geophysical Research*, *83*, 1042–1048. https://doi.org/10.1029/JA083iA03p01042

Streltsov, A. V., & Lotko, W. (2003). Small-scale electric fields in downward auroral current channels. *Journal of Geophysical Research*, *108*, 12890. https://doi.org/10.1029/2002JA009806

Streltsov, A. V., & Lotko, W. (2004). Multiscale electrodynamics of the ionosphere-magnetosphere system. *Journal of Geophysical Research*, *109*, A09214. https://doi.org/10.1029/2004JA010457

Streltsov, A. V., & Lotko, W. (2008). Coupling between density structures, electromagnetic waves and ionospheric feedback in the auroral zone. *Journal of Geophysical Research*, *113*, A05212. https://doi.org/10.1029/2007JA012594

Sydorenko, D., & Rankin, R. (2017). The stabilizing effect of collision-induced velocity shear on the ionospheric feedback instability in Earth's magnetosphere. *Geophysical Research Letters*, *44*, 6534–6542. https://doi.org/10.1002/2017GL073415

Torr, D. G., Torr, M. R., Walker, J. C. G., Nier, A. O., Brace, L. H., & Brinton, H. C. (1976). Recombination of $O_2^+$ in the ionosphere. *Journal of Geophysical Research*, *81*, 5578–5580. https://doi.org/10.1029/JA081i031p05578

Watanabe, T.-H. (2010). Feedback instability in the magnetosphere-ionosphere coupling system: Revisited. *Physics of Plasmas*, *17*, 022904.

Watanabe, T.-H. (2014). A unified model of auroral arc growth and electron acceleration in the magnetosphere-ionosphere coupling. *Geophysical Research Letters*, *41*, 6071–6077. https://doi.org/10.1002/2014GL061166

Watanabe, T.-H., Kurata, H., & Maeyama, S. (2016). Generation of auroral turbulence through the magnetosphere-ionosphere coupling. *New Journal Physics*, *18*, 125010. https://doi.org/10.1088/1367-2630/aa532a

Watanabe, T., Oya, H., Watanabe, K., & Sato, T. (1993). Comprehensive simulation study on local and global development of auroral arcs and field-aligned potentials. *Journal of Geophysical Research*, *98*, 21391–21407. https://doi.org/10.1029/93JA01769

Watanabe, K., & Sato, T. (1988). Self-excitation of auroral arcs in a three-dimensionally coupled magnetosphere-ionosphere system. *Geophysical Research Letters*, *15*, 717–720. https://doi.org/10.1029/GL015i007p00717